Corneal Keratocytes, Fibroblasts, and Myofibroblasts Exhibit Distinct Transcriptional Profiles In Vitro

Kara Poole,[1] Krithika S. Iyer,[2,3] David W. Schmidtke,[2,3] W. Matthew Petroll,[1,3] and Victor D. Varner[2,3]

[1]Department of Ophthalmology, UT Southwestern Medical Center, Dallas, Texas, United States
[2]Department of Bioengineering, University of Texas at Dallas, Richardson, Texas, United States
[3]Department of Biomedical Engineering, UT Southwestern Medical Center, Dallas, Texas, United States

Correspondence: Victor D. Varner, Department of Bioengineering, University of Texas at Dallas, TI-BMES Building, 2336 Inwood Rd., EA3.200B, Dallas, TX 75235, USA; vdv@utdallas.edu or victor.varner@utsouthwestern.edu. W. Matthew Petroll, Department of Ophthalmology, UT Southwestern Medical Center, 5303 Harry Hines Blvd, Fl 6, Dallas, TX 75390; USA; matthew.petroll@utsouthwestern.edu.

KP and KSI contributed equally to this work.

Received: July 5, 2024
Accepted: January 6, 2025
Published: March 12, 2025

Citation: Poole K, Iyer KS, Schmidtke DW, Petroll WM, Varner VD. Corneal keratocytes, fibroblasts, and myofibroblasts exhibit distinct transcriptional profiles in vitro. *Invest Ophthalmol Vis Sci.* 2025;66(3):28. https://doi.org/10.1167/iovs.66.3.28

Purpose. After stromal injury to the cornea, the release of growth factors and proinflammatory cytokines promotes the activation of quiescent keratocytes into a migratory fibroblast and/or fibrotic myofibroblast phenotype. Persistence of the myofibroblast phenotype can lead to corneal fibrosis and scarring, which are leading causes of blindness worldwide. This study aims to establish comprehensive transcriptional profiles for cultured corneal keratocytes, fibroblasts, and myofibroblasts to gain insights into the mechanisms through which these phenotypic changes occur.

Methods. Primary rabbit corneal keratocytes were cultured in either defined serum-free (SF) media, fetal bovine serum (FBS) containing media, or SF media supplemented with TGF-β1 to induce keratocyte, fibroblast, or myofibroblast phenotypes, respectively. Bulk RNA sequencing followed by bioinformatic analyses was performed to identify significant differentially expressed genes (DEGs) and enriched biological pathways for each phenotype.

Results. Genes commonly associated with keratocytes, fibroblasts, or myofibroblasts showed high relative expression in SF, FBS, or TGF-β1 culture conditions, respectively. Differential expression and functional analyses revealed novel DEGs for each cell type, as well as enriched pathways indicative of differences in proliferation, apoptosis, extracellular matrix (ECM) synthesis, cell-ECM interactions, cytokine signaling, and cell mechanics.

Conclusions. Overall, these data demonstrate distinct transcriptional differences among cultured corneal keratocytes, fibroblasts, and myofibroblasts. We have identified genes and signaling pathways that may play important roles in keratocyte differentiation, including many related to mechanotransduction and ECM biology. Our findings have revealed novel molecular markers for each cell type, as well as possible targets for modulating cell behavior and promoting physiological corneal wound healing.

Keywords: corneal stroma, wound healing, RNA sequencing, mechanotransduction, mechanobiology

In their quiescent state, corneal keratocytes are responsible for maintaining the highly organized structure of the stromal extracellular matrix (ECM), which is necessary for corneal transparency.[1,2] Following injury and disruption of the epithelial basement membrane, various inflammatory cytokines and growth factors are released into the stroma and initiate a wound healing response.[3,4] During this process, corneal keratocytes transform into a repair phenotype that involves differentiation into either fibroblasts or myofibroblasts. Corneal fibroblasts are characterized by increased proliferation and migration toward the site of injury,[5,6] whereas myofibroblasts synthesize new ECM and are highly contractile.[7,8] These stromal cell phenotypes are critical components of physiological wound healing[9]; however, in protracted cases, excessive force generation and continued deposition of fibrotic ECM by myofibroblasts can disrupt the stromal architecture, leading to corneal haze and a loss of visual acuity.[10,11]

To study these stromal cell phenotypes in vitro, three distinct culture models have been established experimentally: (1) primary corneal keratocytes cultured in defined serum-free (SF) media to maintain a quiescent phenotype, (2) keratocytes cultured with fetal bovine serum (FBS) to transform them into corneal fibroblasts, and (3) keratocytes cultured in SF media supplemented with TGF-β1 to induce myofibroblast differentiation.[8] Using these culture conditions, previous studies have investigated the many phenotypic differences among keratocytes, fibroblasts, and myofibroblasts, with several focusing on differences in the morphology, motility, and mechanical behavior of these cells.[12–14] Many of these studies have highlighted the importance of cell-ECM interactions, indicating how the composition, structure, and mechanical properties of the ECM can regulate cell contractility, migration, and ECM remodeling.[15–17] For example, the TGF-β1-induced differentiation of myofibroblasts from quiescent corneal keratocytes is

highly sensitive to changes in ECM stiffness.[18] However, it is still unclear how these cells sense and transduce these biomechanical signals into changes in differentiation and behavior.

An investigation of the global transcriptional profile associated with each of these cell types could offer important information on the changes in gene expression associated with keratocyte differentiation into fibroblasts and myofibroblasts. Such an approach also offers the potential to pinpoint new target molecules within the signaling pathways that precede each of these phenotypic changes. Here, we used bulk RNA sequencing (RNA-seq) to establish comprehensive transcriptional profiles for cultured corneal keratocytes (SF), fibroblasts (FBS), and myofibroblasts (TGF-β1). Differential gene expression and functional analyses provided new insight into the mechanisms that regulate each of these cell phenotypes. Of particular interest, we identified several differentially expressed genes and pathways related to cell biomechanics and ECM remodeling.

Methods

Isolation and Cell Culture of Primary Rabbit Keratocytes

Normal rabbit keratocytes (NRKs) were isolated from young New Zealand white rabbit eyes (approximately 8–12 weeks old; Pel-Freez Biologicals, Rogers, AR, USA) and cultured as described previously.[8] Briefly, after removing the epithelium and endothelium, dissected corneas were digested overnight at 37°C in culture media containing 2.0 mg/mL collagenase (Gibco, Grand Island, NY, USA) and 0.5 mg/mL hyaluronidase (Worthington Biochemical Corporation, Lakewood, NJ, USA; 15 corneas per 10 mL media). The isolated cells were then centrifuge-pelleted (4 minutes at 526 × g), resuspended in defined SF media containing Dulbecco's modified Eagle's medium (DMEM; Sigma-Aldrich, St. Louis, MO, USA) supplemented with 100 µM non-essential amino acids (Gibco, Grand Island, NY, USA), 100 µg/mL ascorbic acid (Sigma-Aldrich, St. Louis, MO, USA), 1% RPMI vitamins solution (Sigma-Aldrich, St. Louis, MO, USA), and 1% antibiotic antimycotic solution (Sigma-Aldrich, St. Louis, MO, USA), and plated in 25 cm^2 tissue culture flasks. After 4 days of SF culture, first passage NRKs were plated at a density of 30,000 cells/mL on glass coverslips coated with 50 µg/mL type I collagen (Advanced BioMatrix, Carlsbad, CA, USA). The cells were allowed to attach to the substrates over 24 hours, then, the culture media was swapped for either defined SF media, SF media supplemented with 5 ng/mL TGF-β1 (Sigma-Aldrich, St. Louis, MO, USA), or DMEM containing 10% FBS (Sigma-Aldrich, St. Louis, MO, USA). The cells were then cultured for 5 days (with a media swap at 48 hours) for both SF and TGF-β1 conditions or for 3 days following exposure to FBS to account for the increased proliferation rate in this condition.

RNA Isolation and Sequencing

Eight samples of total RNA were collected for each culture condition using the Aurum Total RNA Mini Kit (Bio-Rad, Hercules, CA, USA). Briefly, cells on collagen-coated glass coverslips were washed twice with sterile phosphate-buffered saline (PBS) and lysed using Aurum Total RNA Lysis Solution. The lysate was collected into sterile 1.5 mL tubes and mixed with RNase-Free 70% ethanol before being added to Aurum RNA-Binding Mini Columns. According to the manufacturer's instructions, a series of centrifugation and low- and high-stringency solution washing steps were performed before eluting the RNA from the columns using molecular biology grade water. The concentration and purity of each sample was confirmed using a Thermo Scientific NanoDrop One. For each culture condition, two experimental replicates (with 2 biological and 2 technical replicates for each experiment) were sent to Novogene Co. (Sacramento, CA, USA) for bulk RNA-seq on Illumina platforms.

Bioinformatic Analysis

Initial bioinformatic analysis performed by Novogene included sample and data quality control, mapping to the reference genome (Hisat2 version 2.0.5), gene expression quantification (featureCounts version 1.5.0-p3), differential expression analysis (DESeq2 R package version 1.20.0), and enrichment analysis (clusterProfiler R package version 3.8.1). The reference genome used for sequence mapping was generated by the McDermott Center Next Generation Sequencing Core at UT Southwestern Medical Center (Dallas, TX, USA).

Gene Expression Quantification. Fragments per kilobase of transcript per million fragments mapped (FPKM) values were calculated based on the length and read count mapped to each gene. FPKM considers the effects of both sequencing depth and gene length and is currently the most common method for estimating gene expression levels. Principal component analysis (PCA) was performed in MATLAB using FPKM values to compare the clustering of samples and culture conditions. PCA is the method of algebraically reducing the dimensionality and extracting significant components from several gene variables to evaluate differences within a group and between different groups in a set of samples.[19]

Differential Expression Analysis. Differential expression analysis was performed for the following comparisons: FBS versus SF, TGF-β1 versus FBS, and TGF-β1 versus SF. Parametric analysis of variance (ANOVA) with Benjamini-Hochberg False Discovery Rate correction at $P = 0.05$ was performed on normalized data to identify genes that were significantly differentially expressed between groups (adjusted P value ≤ 0.05 and absolute value of $|\log_2[\text{fold change}]| \geq 1$). Heatmaps were created in GraphPad Prism using normalized, $\log_2$-transformed FPKM values ($\log_2[\text{FPKM}+1]$) to display relative expression levels across samples (columns) for sets of differentially expressed genes (rows). To normalize expression levels, each sample's gene expression value was adjusted by subtracting the average expression of that gene across all samples, then dividing the result by the standard deviation of the gene's expression. In addition, bar plots showing average FPKM values among the different culture conditions were generated for selected genes of interest.

Enrichment Analysis. Sets of significant differentially expressed genes were further analyzed through Kyoto Encyclopedia of Genes and Genomes (KEGG) enrichment analysis, and pathways with adjusted P value < 0.05 were considered significantly enriched. Bar plots were generated in GraphPad Prism to visualize pathway significance, the number of up- or downregulated genes associated with each pathway, and the BRITE functional hierarchies under

Investigative Ophthalmology & Visual Science

which each pathway is classified. For a subset of significantly enriched KEGG pathways, volcano plots were generated in GraphPad Prism to visualize the significance and $\log_2$(fold change) of individual genes.

Fluorescence Microscopy

In other experiments, samples were fixed and stained for fluorescence microscopy. Additional substrates for each culture condition were used for F-actin and nuclei labeling and immunostaining for fibronectin, vimentin, or α-SMA to observe cytoskeletal organization, morphological changes, and the presence of markers commonly associated with each phenotype. Cells were fixed in 3% paraformaldehyde in PBS for 10 minutes at room temperature, washed 3 times with PBS, then permeabilized in 0.5% Triton X-100 in PBS for 15 minutes. The samples were then blocked with 1% bovine serum albumin fraction V (Equitech-Bio, Kerrville, TX, USA) in PBS for 1 hour at room temperature and incubated overnight at 4°C with the primary antibody solution. The following primary antibodies were used: anti-fibronectin (1:200 dilution; sc-18825; Santa Cruz Biotechnology, Dallas, TX, USA), anti-vimentin (1:200 dilution; sc-6260; Santa Cruz Biotechnology, Dallas, TX, USA), and anti-α-SMA (1:250 dilution; A5228; Sigma-Aldrich, St. Louis, MO, USA). After washing 3 times, the samples were then incubated with Alexa Fluor conjugated secondary antibody, as well as Alexa Fluor 546 phalloidin (Invitrogen, Waltham, MA, USA) for 2 hours at room temperature, followed by 4′-6-diamidino-2-phenylindole (DAPI; Invitrogen, Waltham, MA, USA) for 20 minutes. Imaging was performed on a Zeiss LSM 800 laser scanning confocal microscope using a 40 ×, NA 1.3, Oil DIC Plan-Apochromat objective.

Western Blotting

In other experiments, after rinsing twice with ice-cold, sterile PBS, protein was collected from cells cultured in SF, FBS, or TGF-β1 conditions using a lysis buffer solution containing Pierce RIPA Buffer and Halt Protease and Phosphatase Inhibitor Cocktail (Thermo Scientific, Waltham, MA, USA). Sample lysates were mixed for 30 minutes at 4°C, then centrifuged at 10,000 × g for 10 minutes at 4°C. Protein concentrations were measured using the Microplate BCA Protein Assay Kit (Thermo Scientific, Waltham, MA, USA) to determine load volumes for 5 µg of total protein. Protein samples were subjected to SDS-PAGE electrophoresis using Bio-Rad Mini-PROTEAN TGX Gels, then transferred to PVDF membranes (Bio-Rad, Hercules, CA, USA). Membranes were stained for total protein using Ponceau S (Sigma-Aldrich, St. Louis, MO, USA) and subsequently probed with primary antibody followed by an anti-mouse IgG HRP-linked antibody (Cell Signaling, Danvers, MA, USA). The following primary antibodies were used: anti-aldehyde dehydrogenase 1-A1 (1:1000 dilution; sc-374149; Santa Cruz Biotechnology, Dallas, TX, USA), anti-vimentin (1:1000 dilution; sc-6260; Santa Cruz Biotechnology, Dallas, TX, USA), or anti-α-SMA (1:1000 dilution; A5228; Sigma-Aldrich, St. Louis, MO, USA). Colorimetric (total protein) or chemiluminescence (target protein) imaging was performed using a GE Healthcare Amersham Imager 600 Series. In all cases, Image Studio software (version 5.2.5) was used to quantify protein expression and the amount of target protein was normalized to the amount of total protein. Statistical analysis was performed using GraphPad Prism 10. A one-way ANOVA with a Tukey post hoc test was used to compare group means, and a P value of less than 0.05 was considered statistically significant. A Shapiro-Wilk test was performed prior to each ANOVA to confirm the normality of the data.

Results

Distinct Transcriptional Profiles Characterize Corneal Keratocytes in SF, FBS, and TGF-β1 Culture Conditions

We conducted bulk RNA-seq experiments using primary NRKs cultured in defined SF media, or in the presence of either FBS or exogenous TGF-β1. As observed previously, the cells exhibited a dendritic morphology in SF conditions, an elongated morphology in FBS-containing media, and a broad morphology with visible stress fibers in the presence of TGF-β1 (Fig. 1A).[8,13] PCA showed distinct transcriptional differences between conditions, whereas sample replicates clustered closely, indicating their discrete expression profiles (Fig. 1B). Differential expression analysis showed FBS versus SF contained the highest number of differentially expressed genes (DEGs) at 7693, followed by TGF-β1 versus FBS at 5704, and TGF-β1 versus SF at 4430 (Fig. 1C). Cumulatively, 3174 genes were differentially expressed if both FBS- and TGF-β1-treated cells were compared with SF, whereas 1311 genes were differentially expressed among all 3 groups.

We also observed distinct differences in the number of up- and downregulated DEGs when pairwise comparisons were made between culture conditions (Fig. 1D). A heatmap of DEGs among all groups further indicated distinct transcriptional profiles associated with each culture condition (Fig. 1E). Approximately 50% of these DEGs had high relative expression in SF, whereas 28% and 22% showed high expression in FBS and TGF-β1, respectively. Thus, the principal component, gene count, and differential expression analyses illustrate distinct and significant differential gene expression patterns between keratocytes cultured in SF media, FBS, or TGF-β1. A comprehensive list of the DEGs identified in our analysis, as well as the $\log_2$(fold change) and adjusted P value for each DEG, has been included as Supplementary Dataset S1.

Markers Associated With Keratocytes, Fibroblasts, and Myofibroblasts Are Differentially Expressed Between Culture Conditions

We then compared our transcriptional data with molecular markers known to be associated with corneal keratocytes, fibroblasts, and myofibroblasts. Proteoglycans and corneal crystallins known to be important for corneal transparency,[2,20] such as keratocan (KERA), mimecan (OGN), decorin (DCN), lumican (LUM), aldehyde dehydrogenase 1 family member A1 (ALDH1A1), and transketolase (TKT), showed high relative expression in SF culture (Fig. 2A). Analysis of Western blot data confirmed elevated ALDH1A1 levels when comparing SF to either FBS or TGF-β1 (Fig. 2B).

Following injury, corneal fibroblasts exhibit a proliferative and migratory phenotype, so we then compared expression levels for genes associated with proliferation and cell-ECM interactions in FBS-treated cells. We observed signif-

Investigative Ophthalmology & Visual Science

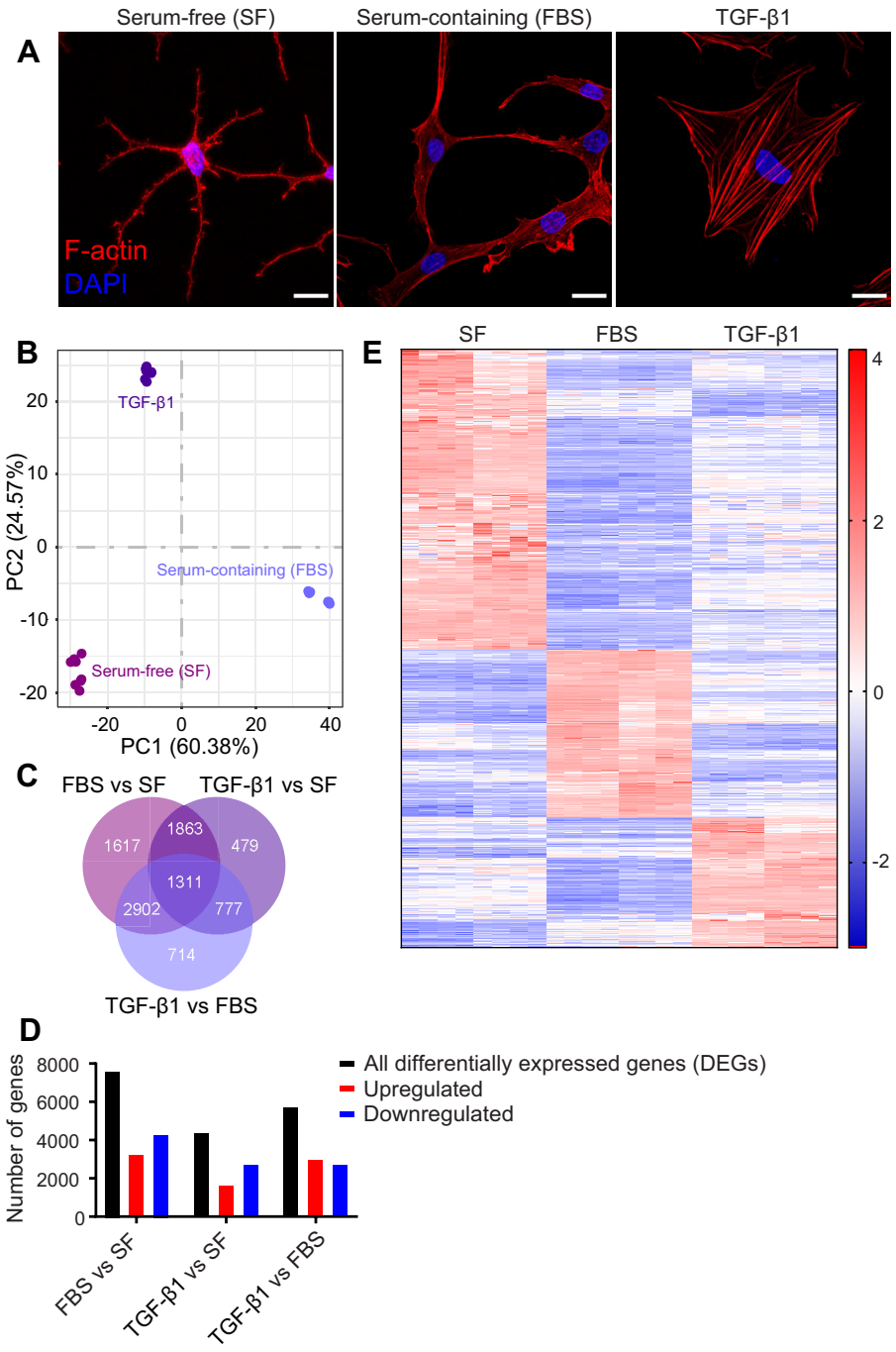

Figure 1. Distinct transcriptional profiles characterize corneal keratocytes in SF, FBS, and TGF-β1 culture conditions. (**A**) Characteristic confocal images of fixed keratocytes cultured in serum-free (SF) media, FBS-containing media, or SF media supplemented with exogenous TGF-β1. Cells were stained with phalloidin (*red*) and DAPI (*blue*) to visualize F–actin and nuclei, respectively. (**B**) Principal component analysis (PCA) of transcriptional differences between corneal keratocytes cultured in SF, FBS, or TGF-β1 culture conditions. Principal component (PC) 1 and PC2, account for 60.38% and 24.57%, respectively, of the variability among these groups. Analysis was performed using normalized, $\log_2$-transformed FPKM values. (**C**) Venn diagram showing the number of significant differentially expressed genes (DEGs) in each comparison. DEGs with an adjusted *P* value (adj *P* value) ≤ 0.05 and $|\log_2[\text{fold change}]| \geq 1$ were considered significant. (**D**) Bar plot depicting the number of DEGs either up- or downregulated in each comparison. (**E**) Heatmap of normalized, $\log_2$-transformed FPKM values ($\log_2$[FPKM+1]) for genes that were differentially expressed across all three culture conditions. *Red color* indicates genes with high relative expression levels, and *blue color* indicates genes with lower expression levels.

icant increases in the expression of proliferative markers, such as Ki-67 (MKI67)[5,21] and proliferating cell nuclear antigen (PCNA),[22,23] as compared to either SF or TGF-β1 (see Fig. 2A). In addition, genes encoding vimentin (VIM),[24] a cytoskeletal intermediate filament, and tenascin C (TNC),[25] an ECM protein synthesized in repair tissue, also exhibited elevated expression following treatment with FBS. Western blots and immunofluorescence labeling confirmed increased

Investigative Ophthalmology & Visual Science

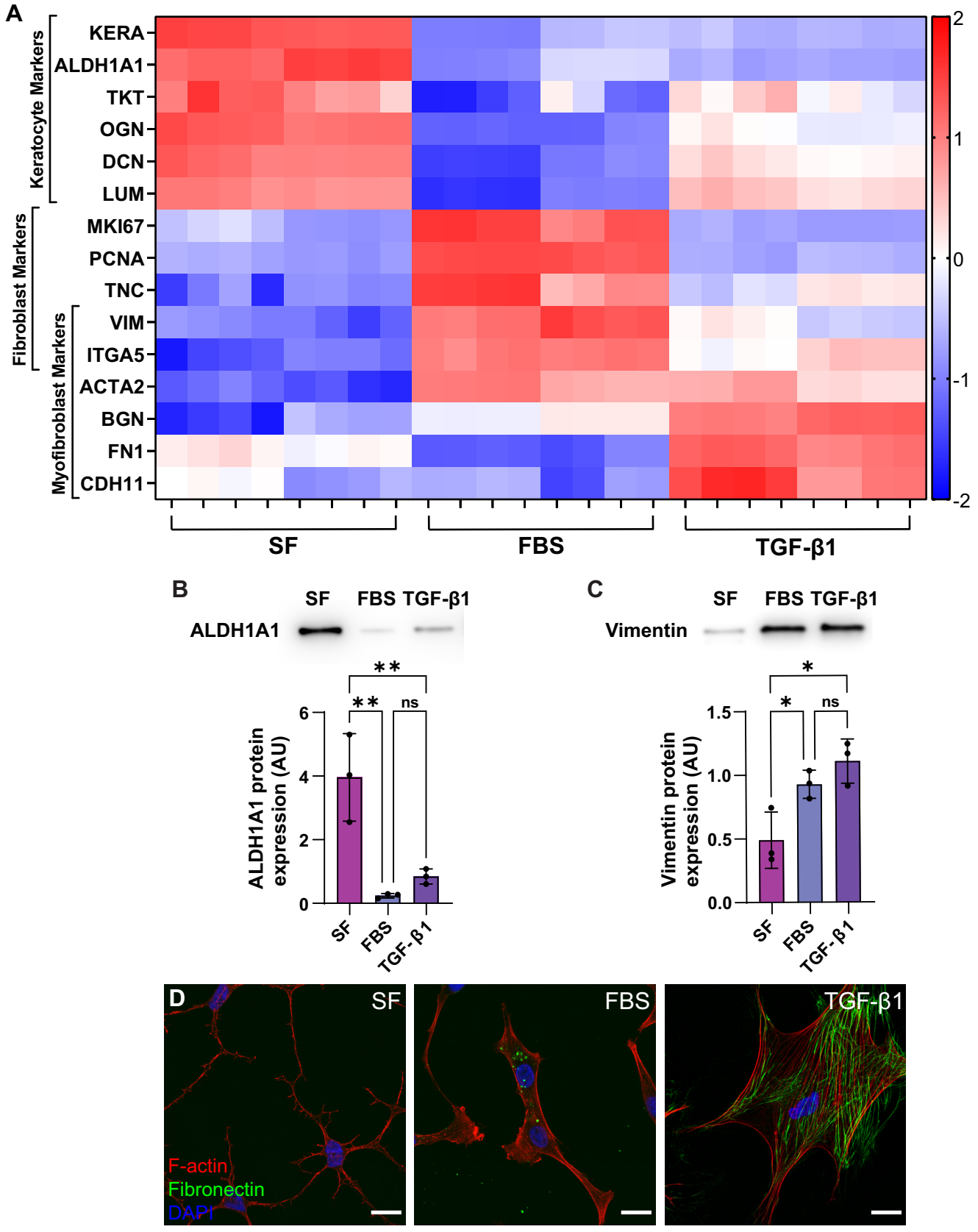

Figure 2. Markers associated with keratocytes, fibroblasts, and myofibroblasts are differentially expressed between culture conditions. (**A**) Heatmap of normalized, $\log_2$-transformed FPKM values ($\log_2$[FPKM+1]) for known keratocyte, fibroblast, and myofibroblast markers. *Red color* indicates genes with high relative expression levels and *blue color* indicates genes with lower expression levels. (**B**, **C**) Representative Western blot and quantification of (**B**) ALDH1A1 as a marker for keratocytes and (**C**) Vimentin as a marker for fibroblasts and myofibroblasts. Quantification of target protein expression was normalized to total protein and reported in arbitrary units (AU). Error

Investigative Ophthalmology & Visual Science

bars represent mean ± SD for 3 experimental replicates. A one-way ANOVA with a Tukey post hoc test was used to compare group means (*, $P < 0.05$; **, $P < 0.01$). (**D**) Confocal images of F-actin, fibronectin, and DAPI staining for corneal keratocytes cultured in SF conditions, or in the presence of FBS or TGF-β1. Scale bar = 20 µm.

levels of VIM in both FBS and TGF-β1-treated cells (Fig. 2C, Supplementary Fig. S1).

We also observed elevated expression of alpha-smooth muscle actin (α-SMA; ACTA2), which incorporates into stress fibers and plays an important role in the increased contractility of myofibroblasts,[26] in both FBS and TGF-β1 as compared to SF (see Fig. 2A). In addition, expression of genes encoding fibrotic ECM proteins, including biglycan (BGN)[27,28] and fibronectin (FN1),[11] were most upregulated upon treatment with TGF-β1. The highest levels of fibronectin protein expression were also observed in the presence of TGF-β1, based on immunofluorescence labeling (Fig. 2D). We also observed increased expression of α5 integrin (ITGA5) in both FBS and TGF-β1 (see Fig. 2A).

Overall, our RNA-seq data are broadly consistent with known molecular markers for corneal keratocytes, fibroblasts, and myofibroblasts, with SF conditions supporting a keratocyte phenotype, FBS-containing media inducing a fibroblast phenotype, and treatment with TGF-β1 eliciting a myofibroblast phenotype. Even so, genes encoding some fibroblast and myofibroblast markers, such as ITGA5 and ACTA2, were expressed at similar levels in both FBS and TGF-β1 culture conditions, indicating overlap between the gene expression profiles of fibroblasts and myofibroblasts.

Diverse Pathways Associated With Signal Transduction and Cellular Processes Such as Cell Growth and Death, Cell-ECM and Cell-Cell Interactions Are Enriched in the Comparisons of Fibroblasts and Myofibroblasts to Keratocytes

KEGG analysis revealed an enrichment of several pathways in TGF-β1-treated myofibroblasts and FBS-treated fibroblasts, when compared with keratocytes in SF conditions (Figs. 3A, 3B). In the presence of FBS, genes were primarily upregulated in pathways related to translation, replication and repair, and cell growth and death. Among these, we observed significant enrichment of the ribosome and ribosome biogenesis pathways, as well as the DNA replication and cell cycle pathways (see Fig. 3A). In addition, significant changes in expression were observed for genes involved in the PI3K-Akt and Rap1 signaling pathways, as well as those associated with ECM-receptor interactions.

In contrast, the focal adhesion, regulation of actin cytoskeleton, ECM-receptor interaction, and Rap1 signaling KEGG pathways were significantly enriched in the comparison of TGF-β1 to SF (see Fig. 3B). Other enriched pathways were broadly related to either cytokine activity (e.g. cytokine-cytokine receptor interaction, as well as TGF-β, JAK-STAT, and TNF signaling pathways) or proliferation and apoptosis (e.g. PI3K-Akt, p53, MAPK, and Hippo signaling pathways).

When TGF-β1-treated myofibroblasts were compared with fibroblasts (as opposed to keratocytes), many of the same KEGG pathways, especially those related to proliferation, cell-ECM interactions, and cytokine activity, were enriched (Fig. 3C). In addition, the cellular senescence pathway was also enriched in this comparison. Taken together, these data were suggestive of lower rates of proliferation and a greater emphasis on cell-ECM interactions in TGF-β1-treated myofibroblasts.

Genes Related to Proliferation and Migration Are Significantly Upregulated in Fibroblasts as Compared to Keratocytes

Numerous genes in the DNA replication, cell cycle, and PI3K-Akt signaling KEGG pathways were differentially expressed in fibroblasts as compared with keratocytes (Figs. 4A–C). Elevated expression was observed for several key genes that encode parts of the DNA replication machinery, including PCNA, MCM2-7, and several DNA polymerase subunits such as POLA2 and POLE2-3.[29] There was also an increase in the expression of several genes associated with the PI3K-Akt signaling pathway, such as the receptor tyrosine kinase MET and the MAP Kinase MAP2K1,[30] and several cyclin dependent kinases (CDKs) such as CDK2 and CDK4.[31] The upregulation of these genes was indicative of an increased proliferative phenotype for cultured corneal fibroblasts.

Numerous DEGs within the Rap1 signaling and ECM-receptor interaction pathways also indicated a shift toward a migratory phenotype (Figs. 4D, 4E). Ras-related protein Rap-1b (RAP1B) encodes for a small GTPase that regulates cell adhesion, migration, and polarity.[32,33] We observed increased expression of RAP1B, along with an upregulation of β-actin (ACTB). In addition, focal adhesion-related genes, such as talin (TLN2), and genes that regulate actin polymerization, like profilin (PFN2),[34] were downregulated following treatment with FBS. Changes in cell-ECM interactions were indicated by shifts in the expression of different integrin subunits and their ECM binding partners. This included the downregulation of various collagens (COL1, COL2, COL4, and COL6) and the upregulation of TNC. Many of the genes encoding integrin subunits that bind to tenascin, such as ITGA8, ITGAV, ITGB1, and ITGB3, were also upregulated. Taken together, these transcriptional changes support an increased proliferative and migratory phenotype in cultured corneal fibroblasts.

Proliferation Related Genes Are Significantly Downregulated, Whereas Genes Involved in Cell-ECM Interactions and Cytokine Signaling Are Upregulated in Myofibroblasts Compared to Fibroblasts

We observed similar differences in proliferation- and motility-related genes when comparing fibroblasts and myofibroblasts. Multiple genes in the DNA replication and cell cycle pathways were differentially expressed between these groups, with lower levels of expression in myofibroblasts (Figs. 5A, 5B). Interestingly, genes involved in cell cycle arrest and evasion of apoptosis, such as the cyclin dependent kinase inhibitors 1A and 2B (CDKN1A and CDKN2B), as well as B-cell lymphoma 2 (BCL2), were upregulated in TGF-β1-treated myofibroblasts (Figs. 5C, 5D).[31,35,36]

Investigative Ophthalmology & Visual Science

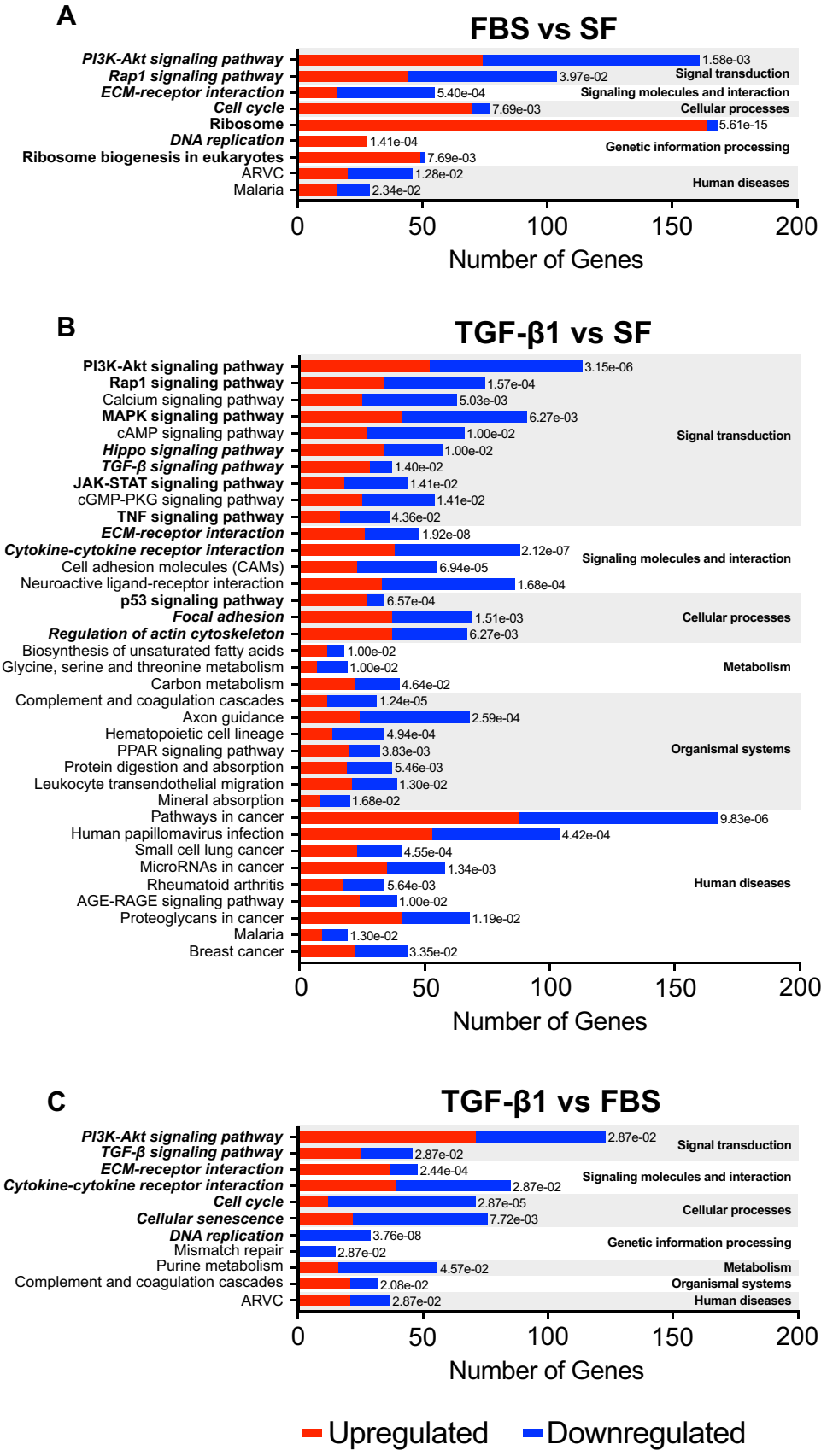

Figure 3. KEGG pathways associated with proliferation are significantly enriched in the comparison of FBS versus SF, whereas pathways associated with signal transduction are enriched in the comparison of TGF-β1 versus SF. Bars represent the number of genes either upregulated (*red*) or downregulated (*blue*) in each significantly enriched KEGG pathway (adj P value < 0.05) from the comparisons

Investigative Ophthalmology & Visual Science

of (**A**) FBS versus SF, (**B**) TGF-β1 versus SF, and (**C**) TGF-β1 versus FBS. In each comparison, KEGG pathways are grouped together based on their associated function, as indicated on the right of each box. Pathways of particular interest are highlighted in bold type.

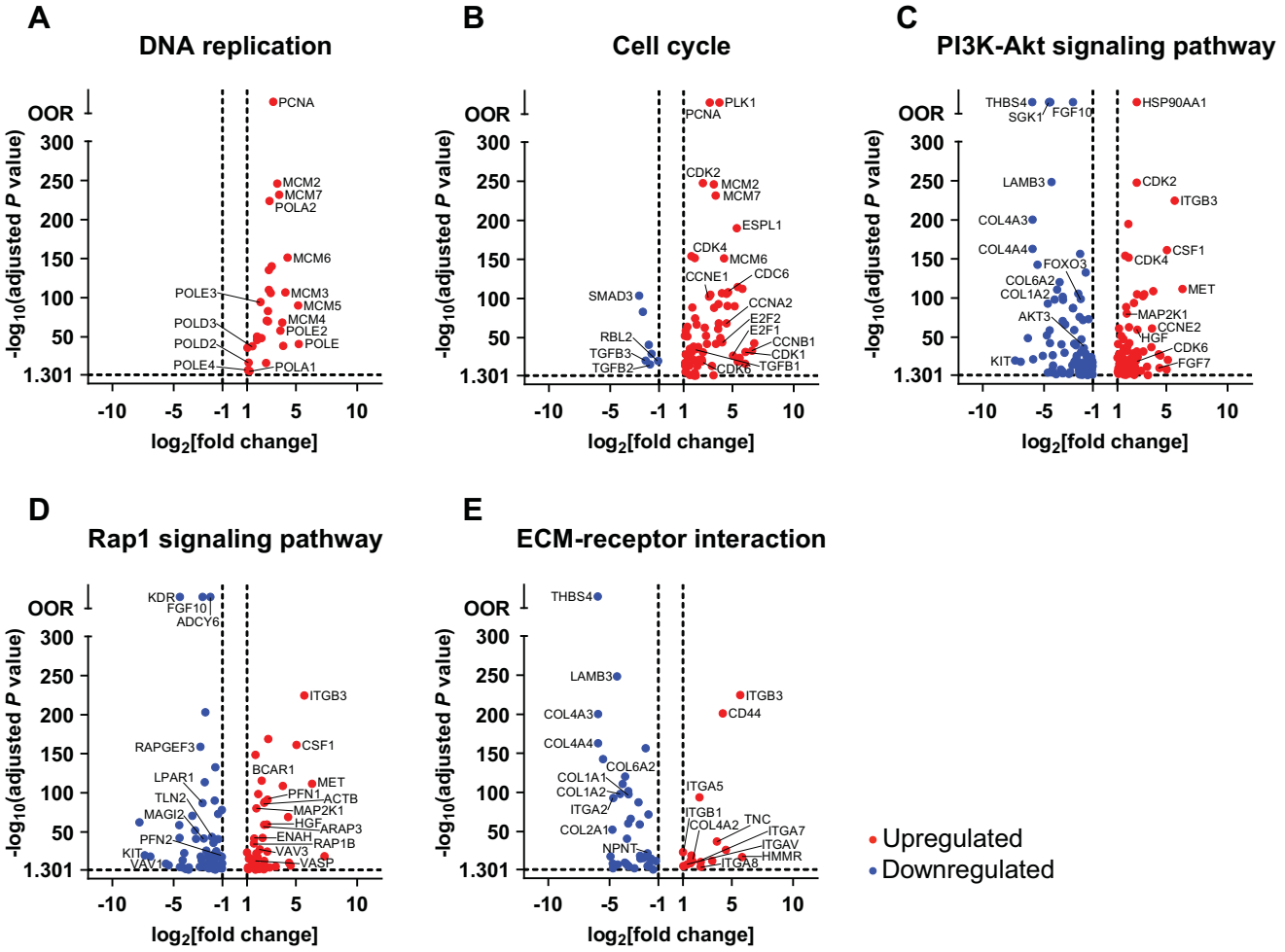

Figure 4. FBS versus SF: genes related to a migratory and proliferative phenotype are significantly upregulated in fibroblasts as compared with quiescent keratocytes. (**A–E**) Volcano plots represent individual genes significantly up- or downregulated within selected KEGG pathways from the comparison of fibroblasts to keratocytes. Genes with adjusted P value ≤ 0.05 (*horizontal dashed line*) and $|\log_2[\text{fold change}]| \geq 1$ (*vertical dashed lines*) were considered significant. *Red dots* indicate genes that were upregulated in fibroblasts, whereas *blue dots* indicate downregulated genes. Genes generally associated with FBS-induced fibroblast phenotypes and several other significant genes with high adjusted P values or fold changes have been labeled.

TGF-β1 has been attributed to the induction of ECM synthesis in myofibroblasts.[37] Here, several ECM genes, including fibronectin (FN1), tenascin N (TNN), various collagens (COL1A1, COL1A2, COL2A1, and COL9A3), and associated integrin subunits (e.g. ITGA11, ITGAV, and ITGB3) exhibited increased expression levels in myofibroblasts compared with fibroblasts (Fig. 5E). Interestingly, the expression of chondroadherin (CHAD), which has been previously shown to promote the adhesion of chondrocytes, fibroblasts, and osteoblasts,[38,39] was highly upregulated in myofibroblasts. In addition, a different gene involved in cell motility – hyaluronan mediated motility receptor (HMMR)[40] – was downregulated in myofibroblasts relative to fibroblasts.

This comparison also revealed significant differences in the expression of genes related to cytokine signaling (Fig. 5F), including several TGF-β family genes (Fig. 5G). We also noted differences in the expression of genes related to cell inflammatory responses, including the interleukins IL-1A, IL-1B, and IL-6, as well as colony stimulating factors CSF1 and CSF3. These genes were downregulated in myofibroblasts as compared with fibroblasts, which are believed to be the cell type responsible for triggering innate immune responses in the cornea.[41] In addition, we observed differential expression of several genes associated with TGF-β signaling, some of which encode proteins that are known to modulate TGF-β activity (see Fig. 5G), including DCN, fibromodulin (FMOD), thrombospondin type 1 domain containing 4 (THSD4), fibrillin 1 (FBN1), and latent transforming growth factor beta binding protein 1 (LTBP1).[42]

Investigative Ophthalmology & Visual Science

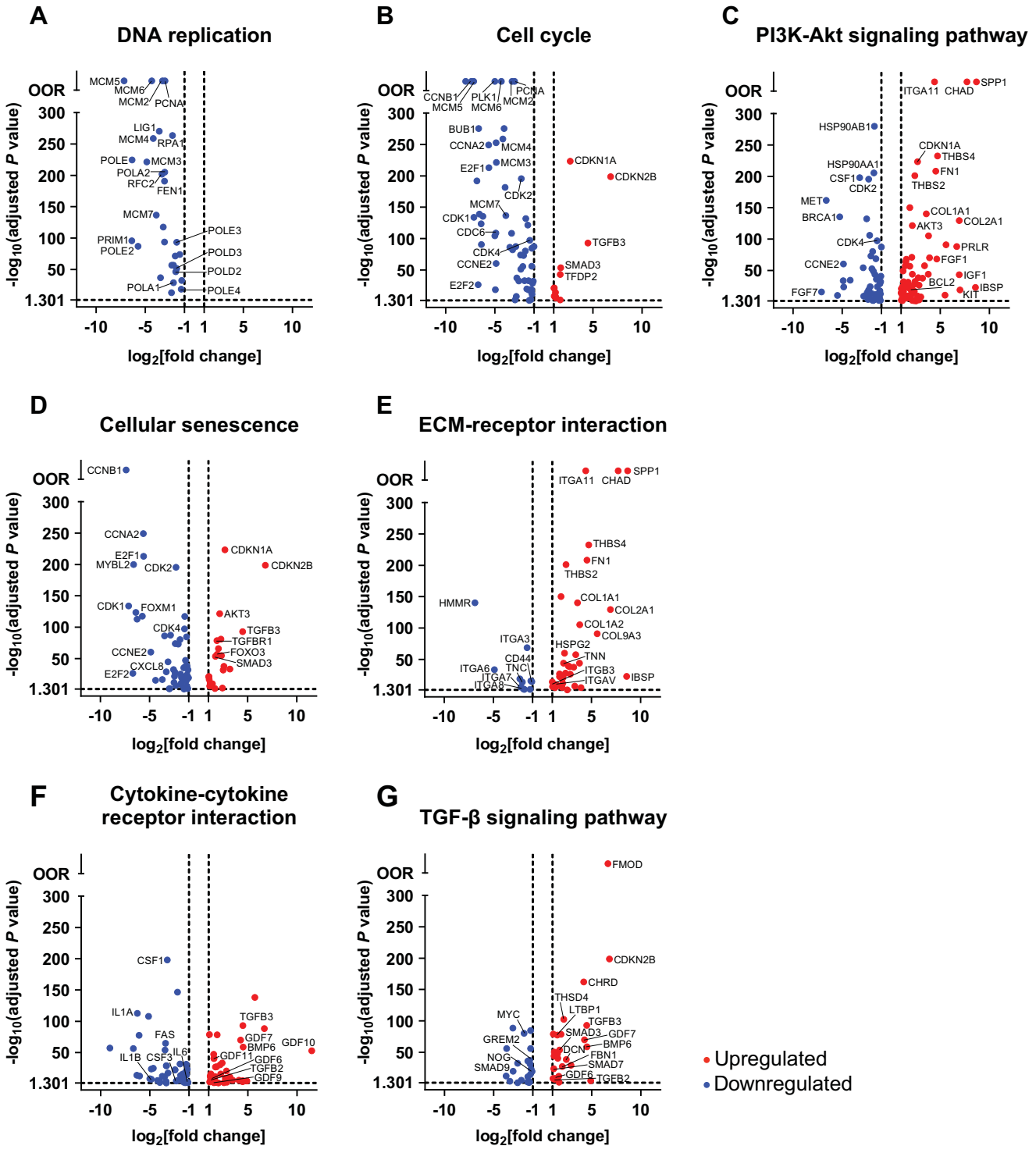

Figure 5. TGF-β1 versus FBS: proliferation related genes are significantly downregulated, and genes involved in cell-ECM interactions and cytokine signaling are upregulated in myofibroblasts compared with fibroblasts. (**A–G**) Volcano plots represent individual genes significantly up- or downregulated within selected KEGG pathways from the comparison of myofibroblasts to fibroblasts. Genes with adjusted *P* values ≤ 0.05 (*horizontal dashed line*) and $|\log_2[\text{fold change}]| \geq 1$ (*vertical dashed lines*) were considered significant. *Red dots* indicate genes that were upregulated in myofibroblasts, whereas *blue dots* indicate downregulated genes. Genes generally associated with either TGFβ1- or FBS-induced phenotypes and several other significant genes with high adjusted *P* values or fold changes have been labeled.

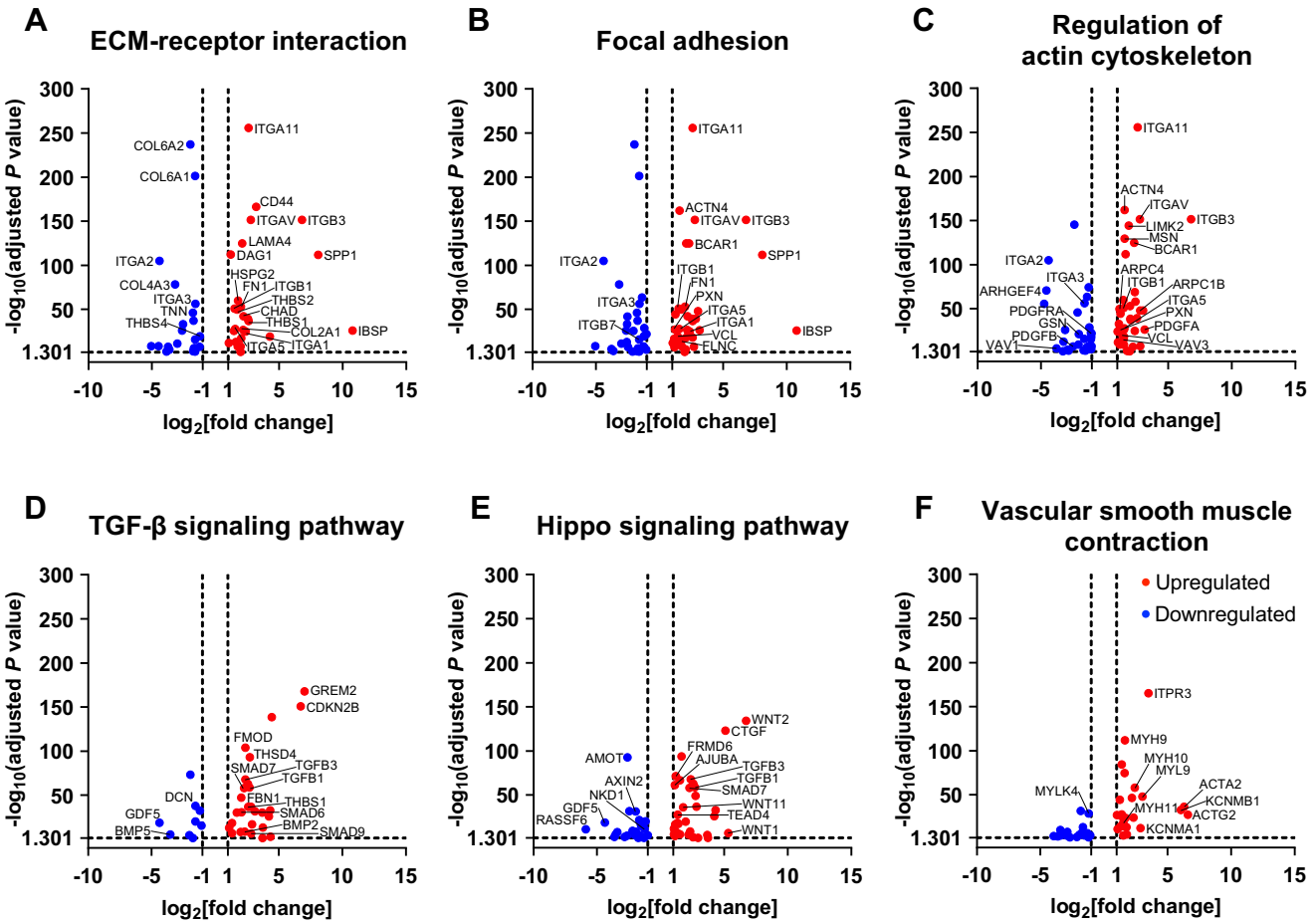

Figure 6. TGF-β1 versus SF: genes in KEGG pathways related to cell-ECM interactions and mechanotransduction are differentially expressed in myofibroblasts compared to keratocytes. **(A–F)** Volcano plots represent individual genes significantly up- or downregulated within selected KEGG pathways from the comparison of myofibroblasts to keratocytes. Genes with adjusted *P* values ≤ 0.05 (*horizontal dashed line*) and $|\log_2[\text{fold change}]| \geq 1$ (*vertical dashed lines*) were considered significant. *Red dots* indicate genes that were upregulated in myofibroblasts, whereas *blue dots* indicate downregulated genes. Genes generally associated with TGF-β1 induced myofibroblast phenotypes and several other significant genes with a high adjusted *P* values or fold changes have been labeled.

Genes Related to Cell-ECM Interactions and Mechanotransduction Are Differentially Expressed in Myofibroblasts Compared With Keratocytes and Fibroblasts

Many of the significantly enriched KEGG pathways identified in the comparison of myofibroblasts to keratocytes were associated with cell-ECM interactions and mechanotransduction (Figs. 6A–E). KEGG enrichment analysis of genes that were significantly upregulated in myofibroblasts also revealed significant enrichment of the vascular smooth muscle contraction pathway (Fig. 6F). Comparison of myofibroblasts to keratocytes identified many DEGs related to ECM, cell-ECM adhesion, cell-cell interaction, Hippo signaling, actomyosin contractility, and growth factor signaling, which were further evaluated for their relative expression across all three culture conditions (Fig. 7A).

Multiple collagens were highly expressed in myofibroblasts compared with keratocytes and fibroblasts. One of the most notable collagens that was significantly upregulated in myofibroblasts was collagen type XI alpha 1 chain (COL11A1; see Figs. 7A, 7B). Interestingly, several other ECM-related genes, such as integrin binding sialoprotein (IBSP), secreted phosphoprotein 1 (SPP1), and leucine rich repeat containing 15 (LRRC15), and integrins such as integrin subunit alpha 11 (ITGA11) were also significantly upregulated in myofibroblasts (see Figs. 7A, 7B, Supplementary Table S1). LRRC15 is a membrane protein known to be involved in ECM binding and as a marker for cancer associated myofibroblasts in lung, breast, and other tumors.[43,44] Our data revealed a very significant upregulation of LRRC15 in the presence of TGF-β1, compared with cells cultured in both SF and FBS conditions.

Among the genes related to growth factor signaling, TGF-β1-treated myofibroblasts exhibited a significant upregulation in TGFB1 and TGFB3 (as compared to SF media; see Fig. 7A). We also observed changes in genes associated with the PDGF pathway. Interestingly, the expression level of PDGFA was upregulated in cultured myofibroblasts, while PDGFB expression was downregulated (see Fig. 7A).

In the comparison of myofibroblasts to keratocytes, DEGs involved in Hippo signaling also stood out due to known crosstalk with TGF-β signaling and its role in mechanotransduction.[45,46] Our data revealed differential expression of several Hippo signaling related genes, including connective tissue growth factor (CTGF) and TEA domain transcription

Investigative Ophthalmology & Visual Science

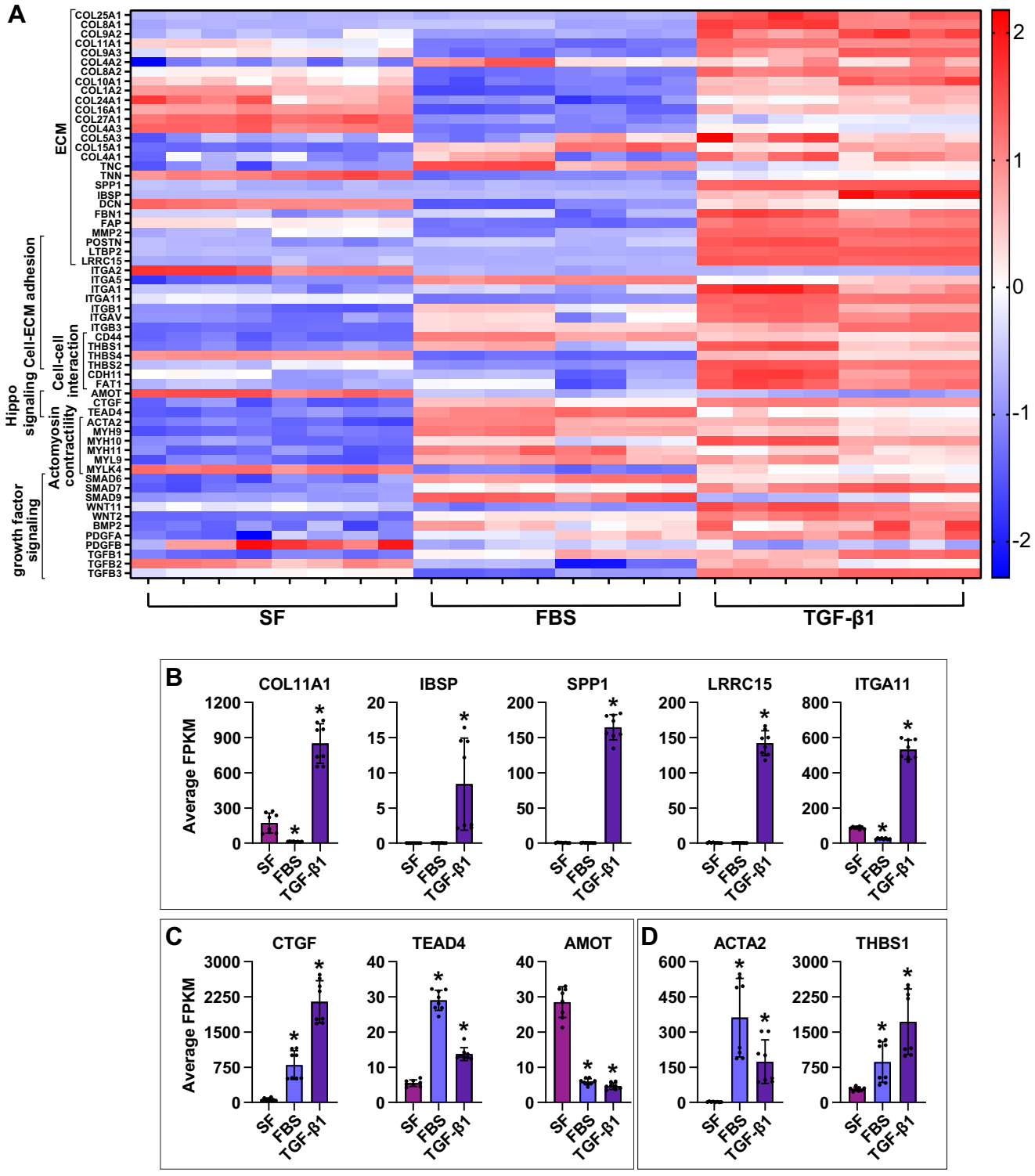

Figure 7. Myofibroblast differentiation is associated with specific ECM and Hippo signaling related genes. (**A**) Heatmap of normalized, $\log_2$-transformed FPKM values ($\log_2$[FPKM+1]) for several genes associated with ECM, cell-cell interactions, Hippo signaling, actomyosin contractility, and growth factor signaling that were differentially expressed in myofibroblasts compared to either keratocytes or fibroblasts. *Red color* indicates genes with high relative expression levels and *blue color* indicates genes with lower expression levels. Selected genes associated with (**B**) ECM, (**C**) Hippo signaling, and (**D**) myofibroblast differentiation have been highlighted in the bar plots. The average FPKM values have been indicated for comparison among the three culture conditions. *Asterisks* indicate if expression levels in either FBS or TGF-β1 conditions were found to be significantly different with respect to SF based on the differential expression analysis (adjusted P value ≤ 0.05 and $|\log_2[\text{fold change}]| \geq 1$).

factor 4 (TEAD4), which were significantly upregulated in myofibroblasts, and angiomotin (AMOT), which was significantly downregulated (see Figs. 7A, 7C).

ACTA2, the gene encoding for α-SMA, was significantly upregulated in both fibroblasts and myofibroblasts, as compared with keratocytes (see Figs. 7A, 7D). TGF-β1-treated myofibroblasts also contained α-SMA positive stress fibers (Supplementary Fig. S2A) and Western blots showed high α-SMA protein levels relative to keratocytes (see Supplementary Fig. S2B). An even higher level of ACTA2 expression, however, was observed for corneal fibroblasts, although we did not observe the incorporation of α-SMA into stress fibers among cells in this culture condition (see Supplementary Fig. S2A), and Western blots showed lower α-SMA protein levels relative to myofibroblasts (see Supplementary Fig. S2B).

Another family of genes differentially expressed in myofibroblasts were the thrombospondins 1, 2, and 4 (THBS 1, 2, and 4), which have the ability to bind to various ECM proteins and modulate cell-ECM and cell-cell interactions[47] (see Fig. 7A). THBS1 specifically was significantly upregulated in myofibroblasts compared with keratocytes (see Figs. 7A, 7D) and is known to be important for TGF-β1-induced myofibroblast differentiation.[48]

Discussion

Although phenotypic differences among corneal keratocytes, fibroblasts, and myofibroblasts have been well documented in vivo and in vitro, less is known about the transcriptional changes that regulate these differences. Improving our understanding of the signaling pathways that influence keratocyte differentiation could have important implications for corneal wound healing and fibrosis. Levels of gene expression have been evaluated previously in mouse corneal stromal cells (in vitro and in vivo) using microarray analysis, with a focus on genes associated with immune activity.[49] Here, we performed bulk RNA-seq to generate a more comprehensive view of the gene expression profiles of cultured primary rabbit corneal keratocytes, fibroblasts, and myofibroblasts. Differential gene expression and functional analyses identified novel molecular markers for each cell type, as well as potential new targets for modulating keratocyte behavior and differentiation. Overall, significant differences in expression were primarily observed for genes involved in cell growth and death, cell-ECM interactions, and cell mechanics.

Fibroblast and Myofibroblast Differentiation Involves Changes in the Expression of Proliferative and Apoptotic Genes

Following injury or surgery, the transformation of quiescent keratocytes into proliferative and migratory fibroblasts is an integral step during corneal wound healing.[50] Our RNA-seq data suggest that increased proliferation observed among corneal fibroblasts is associated with the upregulation of genes involved in the DNA replication, cell cycle, and PI3K-Akt signaling pathways, such as E2F1/2 and CDK2/4/6. These genes, as well as their associated signaling pathways, may be of further interest as potential targets for accelerating cell repopulation during wound healing or promoting stromal regeneration.[51]

Although myofibroblast differentiation is important for proper wound closure, a persistent myofibroblast phenotype can lead to protracted corneal fibrosis.[37,50] Our transcriptional analyses indicated that genes associated with proliferation are downregulated among corneal myofibroblasts. These cells also adopted an apoptotic-resistant phenotype associated with pathological wound healing,[52] as indicated by changes in the cell cycle, cellular senescence, PI3K-Akt, and p53 signaling pathways. Genes of interest within these pathways included BCL2, which was upregulated in myofibroblasts. BCL2 suppresses apoptosis and has been studied for its therapeutic potential in cancer and wound healing.[36,53,54] Indeed, the evasion of apoptosis is considered a distinguishing hallmark of fibrotic disease.[52,55] Targeting genes related to apoptosis during corneal wound healing could be used to support the timely disappearance of myofibroblasts following wound closure.

Cell-ECM Interactions Are an Important Regulator of Fibroblast and Myofibroblast Differentiation

ECM synthesis and remodeling by corneal keratocytes is important for maintaining the optical transparency of the tissue. This ECM-maintenance phenotype is disrupted when keratocytes differentiate into fibroblasts and myofibroblasts.[56] Although previous studies have identified some of the collagens and proteoglycans that are differentially expressed among these cell types, our data provide a more comprehensive profile of ECM-related genes, including ECM structural proteins, integrin subunits, ECM-modifying enzymes, and ECM-binding growth factors and cytokines. Our transcriptional data indicate that the expression of various keratocyte-associated proteoglycans is reduced in myofibroblasts, whereas the expression of ECM genes associated with fibrosis (e.g. COL3A1 and FN1) is elevated, consistent with previous work.[27,56] Our analyses also uncovered novel ECM-related genes, such as osteopontin (SPP1 or OPN) and integrin binding sialoprotein (IBSP), that were highly upregulated in myofibroblasts. Each of these genes is associated with bone matrix remodeling, but previous studies have also suggested a role in wound healing and fibrosis in other tissue types.[25,57–59] OPN expression, for instance, is important during the myofibroblast differentiation of both dermal and cardiac fibroblasts,[60,61] and OPN knockout mice exhibit delayed corneal wound healing, which was associated with lower levels of TGF-β1 expression and fewer myofibroblasts.[62]

Changes in ECM composition likely also influence keratocyte differentiation via interactions with integrin-containing receptors. We found TNC and FN1, which have been investigated previously during inflammation, wound healing, and tissue remodeling,[50,59] to be highly expressed in corneal fibroblasts and myofibroblasts, respectively. The TNC modulates cell adhesion and migration via interactions with α8β1 and αvβ1 integrins, which were expressed at high levels in cultured fibroblasts. The coordinated expression of TNC and its associated integrin subunits may support corneal fibroblast migration. In contrast, fibronectin promotes robust cell attachment to the ECM, and previous work has reported increased fibronectin expression in myofibroblasts, as well as changes in the composition and localization of focal adhesions, which are thought to contribute to the elevated contractile phenotype associated with these cells.[18,63] Consistently, we observed an upreg-

Investigative Ophthalmology & Visual Science

ulation of genes encoding focal adhesion proteins, such as vinculin (VCL), talin (TLN2), and paxillin (PXN) among myofibroblasts. Overall, our analyses have identified distinct ECM-related gene expression profiles for corneal keratocytes, fibroblasts, and myofibroblasts and suggest that cell-ECM interactions are important determinants of keratocyte differentiation.

Mechanical Regulation of Corneal Stromal Cell Behavior

Recent work has also highlighted the importance of biophysical cues in regulating corneal stromal cell behavior.[15,64,65] The myofibroblast differentiation of quiescent keratocytes, for instance, is highly sensitive to changes in the mechanical properties of the ECM.[9,18] In the presence of TGF-β1, keratocytes cultured in a soft microenvironment form fewer stress fibers and exhibit lower levels of α-SMA expression, as compared with cells cultured on stiff substrata.[15,66] This decreased level of myofibroblast differentiation is accompanied by lower cell contractility, as well as substantial changes in the subcellular distribution of focal adhesions.[18,63]

Consistent with these data, our RNA-seq analyses identified an enrichment of pathways related to cell contractility and mechanotransduction in TGF-β1-treated myofibroblasts. We observed significant changes in the expression of AMOT, as well as multiple SMADs, which have been shown to influence the activity of the mechanosensory proteins YAP and TAZ.[67] Previous studies have shown that YAP/TAZ signaling can regulate the myofibroblast differentiation of cultured human corneal fibroblasts,[68] and AMOT is known to suppress YAP/TAZ-mediated transcription.[67] The observed downregulation of AMOT in TGF-β1-treated myofibroblasts is suggestive of elevated YAP/TAZ activity, an idea that is also supported by increased CTGF expression, a downstream transcriptional target of YAP.[69]

In addition, α-SMA expression is a key marker for corneal myofibroblasts and can be modulated by changes in the mechanical properties of the ECM.[18,26,66] We observed a significant upregulation of ACTA2, the gene encoding α-SMA, in TGF-β1-treated myofibroblasts. Interestingly, however, we measured even higher levels of ACTA2 expression among corneal fibroblasts. These results may indicate an important transcriptional difference in ACTA2 expression between corneal fibroblasts and myofibroblasts; however, it is also a possibility that time-varying changes in ACTA2 expression contribute to this observation. In addition, our Western blot data indicate that α-SMA protein levels do not necessarily correlate with ACTA2 transcriptional levels when comparing fibroblasts and myofibroblasts, which may indicate potential post-transcriptional or translational control mechanisms.

Previous work has suggested that other signaling pathways, such as those downstream of PDGF, can also influence α-SMA expression. Specifically, it has been shown that TGF-β1 induces the secretion of PDGF as part of an autocrine signaling loop which regulates myofibroblast differentiation.[70] However, the specific PDGF subunits involved in this process are still unknown. Our transcriptional data indicate that PDGFA expression is upregulated in myofibroblasts, whereas the expression of PDGFB decreases.

Taken together, these data represent the first comprehensive transcriptional profile for cultured primary corneal keratocytes, fibroblasts, and myofibroblasts. Our RNA-seq analyses have identified genes and signaling pathways that may play important roles in keratocyte differentiation, as well as the maintenance of each of these distinct cell phenotypes. Going forward, these data will serve as the foundation for future studies investigating the influence of ECM mechanics on corneal keratocyte behavior. These experiments will help uncover specific genes of interest and further reveal the biological and functional significance of these findings as they relate to the broader fields of wound healing, fibrosis, and tissue engineering.

Acknowledgments

The authors thank the members of the Varner, Petroll, and Schmidtke laboratories for their many helpful discussions and comments.

Supported by the National Institutes of Health (NIH) grants R01 EY013322, R01 EY030190, and P30 EY030413, as well as a Challenge grant from Research to Prevent Blindness.

Author Contributions: K.P., K.S.I., V.D.V., W.M.P., and D.W.S. conceived the study and designed experiments. K.P. and K.S.I. conducted all experiments and analyzed all experimental data. All authors discussed and interpreted results. K.P., K.S.I., V.D.V., and W.M.P. wrote the manuscript with feedback from all authors.

Data Availability: The data discussed in this publication have been deposited in NCBI's Gene Expression Omnibus and are accessible via the GEO series accession number GSE287915.

Disclosure: **K. Poole**, None; **K.S. Iyer**, None; **D.W. Schmidtke**, None; **W.M. Petroll**, None; **V.D. Varner**, None

References

1. Fini ME. Keratocyte and fibroblast phenotypes in the repairing cornea. *Prog Retin Eye Res*. 1999;18(4):529–551.
2. Meek KM. Corneal collagen-its role in maintaining corneal shape and transparency. *Biophys Rev*. 2009;1(2):83–93.
3. Imanishi J, Kamiyama K, Iguchi I, Kita M, Sotozono C, Kinoshita S. Growth factors: importance in wound healing and maintenance of transparency of the cornea. *Prog Retin Eye Res*. 2000;19(1):113–129.
4. Wilson SE, Mohan RR, Mohan RR, Ambrósio R, Jr, Hong J, Lee J. The corneal wound healing response: cytokine-mediated interaction of the epithelium, stroma, and inflammatory cells. *Prog Retin Eye Res*. 2001;20(5):625–637.
5. Zieske JD, Guimarães SR, Hutcheon AE. Kinetics of keratocyte proliferation in response to epithelial debridement. *Exp Eye Res*. 2001;72(1):33–39.
6. Petroll WM, Kivanany PB, Hagenasr D, Graham EK. Corneal fibroblast migration patterns during intrastromal wound healing correlate with ECM structure and alignment. *Invest Ophthalmol Vis Sci*. 2015;56(12):7352–7361.
7. Myrna KE, Pot SA, Murphy CJ. Meet the corneal myofibroblast: the role of myofibroblast transformation in corneal wound healing and pathology. *Vet Ophthalmol*. 2009;12(Suppl 1):25–27.
8. Jester JV, Barry-Lane PA, Cavanagh HD, Petroll WM. Induction of α-smooth muscle actin expression and myofibroblast transformation in cultured corneal keratocytes. *Cornea*. 1996;15(5):505–516.
9. Pot SA, Lin Z, Shiu J, Benn MC, Vogel V. Growth factors and mechano-regulated reciprocal crosstalk with extracellular matrix tune the keratocyte–fibroblast/myofibroblast transition. *Sci Rep*. 2023;13(1):11350.

10. Wilson SE. Corneal myofibroblast biology and pathobiology: generation, persistence, and transparency. *Exp Eye Res*. 2012;99:78–88.
11. Jester JV, Petroll WM, Cavanagh HD. Corneal stromal wound healing in refractive surgery: the role of myofibroblasts. *Prog Retin Eye Res*. 1999;18(3):311–356.
12. Lakshman N, Kim A, Petroll WM. Characterization of corneal keratocyte morphology and mechanical activity within 3-D collagen matrices. *Exp Eye Res*. 2010;90(2):350–359.
13. Jester JV, Ho-Chang J. Modulation of cultured corneal keratocyte phenotype by growth factors/cytokines control in vitro contractility and extracellular matrix contraction. *Exp Eye Res*. 2003;77(5):581–592.
14. Kim A, Lakshman N, Karamichos D, Petroll WM. Growth factor regulation of corneal keratocyte differentiation and migration in compressed collagen matrices. *Invest Ophthalmol Vis Sci*. 2010;51(2):864–875.
15. Petroll WM, Miron-Mendoza M. Mechanical interactions and crosstalk between corneal keratocytes and the extracellular matrix. *Exp Eye Res*. 2015;133:49–57.
16. Miron-Mendoza M, Graham E, Kivanany P, Quiring J, Petroll WM. The role of thrombin and cell contractility in regulating clustering and collective migration of corneal fibroblasts in different ECM environments. *Invest Ophthalmol Vis Sci*. 2015;56(3):2079–2090.
17. Lakshman N, Petroll WM. Growth factor regulation of corneal keratocyte mechanical phenotypes in 3-D collagen matrices. *Invest Opthalmol Vis Sci*. 2012;53(3):1077–1086.
18. Maruri DP, Miron-Mendoza M, Kivanany PB, et al. ECM stiffness controls the activation and contractility of corneal keratocytes in response to TGF-β1. *Biophys J*. 2020;119(9):1865–1877.
19. Ringnér M. What is principal component analysis? *Nat Biotechnol*. 2008;26(3):303–304.
20. Jester JV. Corneal crystallins and the development of cellular transparency. *Semin Cell Dev Biol*. 2008;19(2):82–93.
21. Scholzen T, Gerdes J. The Ki-67 protein: from the known and the unknown. *J Cell Physiol*. 2000;182(3):311–322.
22. Binte M, Yusoff NZ, Riau AK, et al. Isolation and propagation of human corneal stromal keratocytes for tissue engineering and cell therapy. *Cells*. 2022;11(1):178.
23. Gan L, Fagerholm P, Ekenbark S. Expression of proliferating cell nuclear antigen in corneas kept in long term culture. *Acta Ophthalmol Scand*. 1998;76(3):308–313.
24. Wilson SE. The yin and yang of mesenchymal cells in the corneal stromal fibrosis response to injury: the cornea as a model of fibrosis in other organs. *Biomolecules*. 2022;13(1):87.
25. Sumioka T, Matsumoto KI, Reinach PS, Saika S. Tenascins and osteopontin in biological response in cornea. *Ocul Surf*. 2023;29:131–149.
26. Jester JV, Petroll WM, Barry PA, Cavanagh HD. Expression of α-smooth muscle (α-SM) actin during corneal stromal wound healing. *Invest Ophthalmol Vis Sci*. 1995;36(5):809–819.
27. Funderburgh JL, Funderburgh ML, Mann MM, Corpuz L, Roth MR. Proteoglycan expression during transforming growth factor beta -induced keratocyte-myofibroblast transdifferentiation. *J Biol Chem*. 2001;276(47):44173–44178.
28. Massoudi D, Malecaze F, Galiacy SD. Collagens and proteoglycans of the cornea: importance in transparency and visual disorders. *Cell and Tissue Research*. 2016;363(2):337–349.
29. Waga S, Stillman B. The DNA replication fork in eukaryotic cells. *Annu Rev Biochem*. 1998;67:721–751.
30. Organ SL, Tsao MS. An overview of the c-MET signaling pathway. *Ther Adv Med Oncol*. 2011;3(1 Suppl):S7–S19.
31. Łukasik P, Załuski M, Gutowska I. Cyclin-dependent kinases (CDK) and their role in diseases development-review. *Int J Mol Sci*. 2021;22(6):2935.
32. Bos JL. Linking Rap to cell adhesion. *Curr Opin Cell Biol*. 2005;17(2):123–128.
33. Wilson JM, Prokop JW, Lorimer E, Ntantie E, Williams CL. Differences in the phosphorylation-dependent regulation of prenylation of Rap1A and Rap1B. *J Mol Biol*. 2016;428(24 Pt B):4929–4945.
34. Ding Z, Roy P. Profilin-1 versus profilin-2: two faces of the same coin? *Breast Cancer Res*. 2013;15(3):311.
35. Reed JC. Bcl-2 and the regulation of programmed cell death. *J Cell Biol*. 1994;124(1-2):1–6.
36. Ruvolo PP, Deng X, May WS. Phosphorylation of Bcl2 and regulation of apoptosis. *Leukemia*. 2001;15(4):515–522.
37. Wilson SE. Corneal myofibroblasts and fibrosis. *Exp Eye Res*. 2020;201:108272.
38. Mizuno M, Fujisawa R, Kuboki Y. Bone chondroadherin promotes attachment of osteoblastic cells to solid-state substrates and shows affinity to collagen. *Calcif Tissue Int*. 1996;59(3):163–167.
39. Camper L, Heinegârd D, Lundgren-Akerlund E. Integrin alpha2beta1 is a receptor for the cartilage matrix protein chondroadherin. *J Cell Biol*. 1997;138(5):1159–1167.
40. Tolg C, McCarthy JB, Yazdani A, Turley EA. Hyaluronan and RHAMM in wound repair and the "cancerization" of stromal tissues. *Biomed Res Int*. 2014;2014:103923.
41. Fukuda K. Corneal fibroblasts: function and markers. *Exp Eye Res*. 2020;200:108229.
42. Soo C, Hu FY, Zhang X, et al. Differential expression of fibromodulin, a transforming growth factor-beta modulator, in fetal skin development and scarless repair. *Am J Pathol*. 2000;157(2):423–433.
43. Purcell JW, Tanlimco SG, Hickson J, et al. LRRC15 is a novel mesenchymal protein and stromal target for antibody-drug conjugates. *Cancer Res*. 2018;78(14):4059–4072.
44. Krishnamurty AT, Shyer JA, Thai M, et al. LRRC15(+) myofibroblasts dictate the stromal setpoint to suppress tumour immunity. *Nature*. 2022;611(7934):148–154.
45. Attisano L, Wrana JL. Signal integration in TGF-β, WNT, and Hippo pathways. *F1000Prime Rep*. 2013;5:17.
46. Chang YC, Wu JW, Wang CW, Jang ACC. Hippo signaling-mediated mechanotransduction in cell movement and cancer metastasis. *Front Mol Biosci*. 2019;6:157.
47. Lahav J. The functions of thrombospondin and its involvement in physiology and pathophysiology. *Biochim Biophys Acta*. 1993;1182(1):1–14.
48. Bradshaw AD. Chapter 15 - Regulation of cell behavior by extracellular proteins. In Lanza R., Langer R., Vacanti J., Eds. *Principles of Tissue Engineering* (Fourth Edition). Boston, MA: Academic Press; 2014:279–290.
49. Chakravarti S, Wu F, Vij N, Roberts L, Joyce S. Microarray studies reveal macrophage-like function of stromal keratocytes in the cornea. *Invest Ophthalmol Vis Sci*. 2004;45(10):3475–3484.
50. Kamil S, Mohan RR. Corneal stromal wound healing: major regulators and therapeutic targets. *Ocul Surf*. 2021;19:290–306.
51. Lagali N. Corneal stromal regeneration: current status and future therapeutic potential. *Curr Eye Res*. 2020;45(3):278–290.
52. Hinz B, Lagares D. Evasion of apoptosis by myofibroblasts: a hallmark of fibrotic diseases. *Nat Rev Rheumatol*. 2020;16(1):11–31.
53. Qian S, Wei Z, Yang W, Huang J, Yang Y, Wang J. The role of BCL-2 family proteins in regulating apoptosis and cancer therapy. *Front Oncol*. 2022;12:985363.

Investigative Ophthalmology & Visual Science

54. Wilkinson HN, Hardman MJ. Senescence in wound repair: emerging strategies to target chronic healing wounds. *Front Cell Dev Biol*. 2020;8:773.
55. Wu YS, Liang S, Li DY, Wen JH, Tang JX, Liu HF. Cell cycle dysregulation and renal fibrosis. *Front Cell Dev Biol*. 2021;9:714320.
56. Funderburgh JL, Mann MM, Funderburgh ML. Keratocyte phenotype mediates proteoglycan structure: a role for fibroblasts in corneal fibrosis. *J Biol Chem*. 2003;278(46):45629–45637.
57. Icer MA, Gezmen-Karadag M. The multiple functions and mechanisms of osteopontin. *Clin Biochem*. 2018;59:17–24.
58. Moorman HR, Poschel D, Klement JD, Lu C, Redd PS, Liu K. Osteopontin: a key regulator of tumor progression and immunomodulation. *Cancers*. 2020;12(11):3379.
59. Saika S, Yamanaka O, Okada Y, Sumioka T. Modulation of Smad signaling by non-TGFβ components in myofibroblast generation during wound healing in corneal stroma. *Exp Eye Res*. 2016;142:40–48.
60. Lenga Y, Koh A, Perera AS, McCulloch CA, Sodek J, Zohar R. Osteopontin expression is required for myofibroblast differentiation. *Circ Res*. 2008;102(3):319–327.
61. Abdelaziz Mohamed I, Gadeau AP, Hasan A, Abdulrahman N, Mraiche F. Osteopontin: a promising therapeutic target in cardiac fibrosis. *Cells*. 2019;8(12):1558.
62. Miyazaki K-I, Okada Y, Yamanaka O, et al. Corneal wound healing in an osteopontin-deficient mouse. *Invest Ophthalmol Vis Sci*. 2008;49(4):1367–1375.
63. Maruri DP, Iyer KS, Schmidtke DW, Petroll WM, Varner VD. Signaling downstream of focal adhesions regulates stiffness-dependent differences in the TGF-β1-mediated myofibroblast differentiation of corneal keratocytes. *Front Cell Dev Biol*. 2022;10:886759.
64. Petroll WM, Varner VD, Schmidtke DW. Keratocyte mechanobiology. *Exp Eye Res*. 2020;200:108228.
65. Karamichos D, Lakshman N, Petroll WM. Regulation of corneal fibroblast morphology and collagen reorganization by extracellular matrix mechanical properties. *Invest Ophthalmol Vis Sci*. 2007;48(11):5030–5037.
66. Dreier B, Thomasy SM, Mendonsa R, Raghunathan VK, Russell P, Murphy CJ. Substratum compliance modulates corneal fibroblast to myofibroblast transformation. *Invest Ophthalmol Vis Sci*. 2013;54(8):5901–5907.
67. Chan SW, Lim CJ, Chong YF, Pobbati AV, Huang C, Hong W. Hippo pathway-independent restriction of TAZ and YAP by angiomotin. *J Biol Chem*. 2011;286(9):7018–7026.
68. Muppala S, Raghunathan VK, Jalilian I, Thomasy S, Murphy CJ. YAP and TAZ are distinct effectors of corneal myofibroblast transformation. *Exp Eye Res*. 2019;180:102–109.
69. Raghunathan VK, Dreier B, Morgan JT, et al. Involvement of YAP, TAZ and HSP90 in contact guidance and intercellular junction formation in corneal epithelial cells. *PLoS One*. 2014;9(10):e109811.
70. Jester JV, Huang J, Petroll WM, Cavanagh HD. TGFβ induced myofibroblast differentiation of rabbit keratocytes requires synergistic TGFβ, PDGF and integrin signaling. *Exp Eye Res*. 2002;75(6):645–657.

Investigative Ophthalmology & Visual Science